Journal of Multidisciplinary Engineering Science and Technology (JMEST)
ISSN: 3159-0040
Vol. 2 Issue 6, June - 2015

Microwave shielding and DC Electrical Properties of Carbon Black Loaded Rubber Nano-Composites

Gamal M. Nasr, Mohammed A. Soliman, Hussam H. Hassan, S. M. Salem-Gaballah
Physics Department, Faculty of Science, Cairo University.
Giza, Egypt

***Abstract*—In this work, ten carbon black (CB) loaded elastic acrylonitrile butadiene rubber (NBR) nano-composites have been prepared to be used in microwave shielding applications. The DC electric properties of these CB loaded NBR composites have been studied. The evolution of DC conductivity of CB loaded NBR composites with loading level revealed S-shapes curve in accordance with the percolation theory. The current (I)-voltage (V) relations have been studied for these samples at room temperature. All CB loaded NBR composite samples showed Ohmic behavior with the exception of two samples namely CB30 and CB40 in which space charge limited conduction is obvious. Microwave shielding has been calculated from the transmittance data measured using terahertz time domain spectroscopy (THz-TDS) technique. The analysis of microwave shielding data revealed that the sample CB70 has the highest shielding effectiveness. The results of the microwave shielding effectiveness of CB loaded NBR composites were correlated to their DC electric conductivities. Results showed that there is a strong relationship between the DC electric conductivity of the samples and their activity regarding microwave shielding effectiveness. The current investigation of microwave shielding properties of CB loaded NBR composites magnifies the importance of DC electric conduction losses as a major mechanism for microwave shielding.**

Keywords—Carbon Black, NBR, microwave, shielding, nano-composites, THz-TDS.

.

I. INTRODUCTION

The emergence of the need for broad band microwave shields that combine in the same time elastic properties, thermal resistance as well as wide range of operation entails the incorporation of various microwave shielding materials as fillers in a rubbery matrix. In particular, rubber nanocomposites have attracted the attention of many researchers due to their unique properties.

In rubber, fillers are used to achieve products with improved properties for end use applications. Rubber based composites can thus find wide range of applications because of their low density and their ability to be molded into various complex shapes that can match different uses. Moreover, the cost of large scale production of rubber blends is relatively small in comparison with other composites [1].

Rubber composites containing conductive nanoscale fillers are attractive for microwave shielding [1]. This is because their physical properties can be easily adjusted by varying the loading level of these fillers. Rubber based microwave shielding composites that contain carbonaceous nanoparticles offer a large flexibility for design and properties control. The shielding properties of such composites can be tailored through changes in geometry, composition, morphology, and volume fraction of the carbon filler [2].

Incorporation of nanoscale carbonaceous fillers in rubbery matrix produces rubber composites that are either dielectric or conductive depending on the nature of the carbon black filler and its concentration [3]. Conductive elastic rubber composites can be synthesized by adding carbon lack filler to an elastic matrix in a concentration that exceeds the percolation threshold. In order for a conductive filler to be highly effective, it preferably should have a small unit size (relative to the skin depth) to enhance microwave penetration deep inside the shield, and high conductivity to increase the dielectric as well as conduction losses.

DC electric conductivity of these rubber composities represents a crucial aspect of their microwave shielding behavior. Thus studies on electrically conducting carbon black loaded polymer composites are of much great interest. This is because nanoscale carbon black can in low loading levels increase the DC conductivity of the NBR by several orders of magnitude [4]. The aforementioned fact is considered greatly important for this study because the shielding behavior depends to a great extent on the electrical properties of the microwave shielding material [5].

Table (1): Composition of CB loaded NBR composites

Ingredients	Role	phr	Specific gravity
NBR	Matrix	100	0.98
Stearic acid	Plasticizer	2	0.940
Zinc oxide	Activator	5	5.58
Processing oil (DOP)*	Processing oil	50	0.98
Lithium ferrite (LF)	Ferromagnetic filler	0, 10, …100	1.3
MBTS*	accelerator	2	1.5
IPPD* 4020	antioxidant	1	0.995
Sulfur	Vulcanizing agent	2	2.05

***DOP** Dioctyl phthalate
MBTS: 2,2'-Dithiobenzothiazole
IPPD: N-Phenyl-N'-isopropyl-p-phenylenediamine
phr : Part per hundred parts of rubber by weight.

The aim of this work is to study the microwave shielding properties of carbon black (N220) loaded NBR composites in a concentration range from 10-100 phr. They are nominated in this article as CB10, CB20,….CB100. Their DC conductivity is aimed to be studied as well in order to find the most effective CB loaded NBR sample that can be used for preparation of magnetodielectric microwave absorbers in further studies.

II. Experimental

a) Preparation of CB loaded NBR composites

CB loaded NBR composites were prepared in accordance with ASTM D3182-07 using a two roll-mixing mill with outside diameter 470 mm, working distance 300 mm, speed of slow roll 24 rpm and fraction ratio of (1:1.4). The compounding ingredients were obtained from the Transport and Engineering Co., Alexandria, Egypt and are enlisted in table (1). Vulcanization was carried out using an electrically heated platen press at 155±2 °C and 4 MPa (150 bar) for the optimum cure time 30 minutes as previously determined from Monsanto Rheometer.

b) DC Electrical Measurements

The dc measurements were carried out using PASCO scientific model 1030A high voltage power supply and Keithly 614 electrometer. The circuit was constructed as shown in figure (1). The samples were molded into pellet shapes of 1cm thickness and 8 mm diameter. They were polished and covered with silver paste on both sides.

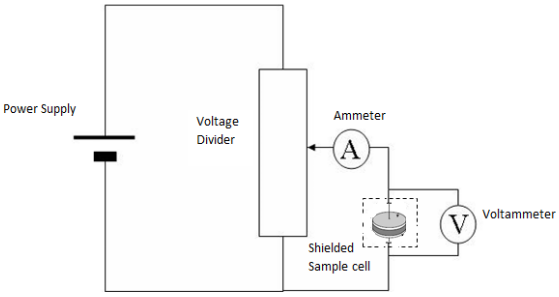

Figure (1): Schematic diagram of the circuit used for DC conductivity and I-V measurements.

The DC electric conductivity (σ) was calculated from:

$$\sigma = \frac{d}{AR} \quad (1)$$

Where d is sample thickness, A its area, and R is the measured resistance.

c) Microwave Shielding Effectiveness measurements

Terahertz time-domain spectroscopy system (THz-TDS) of the type (TPS Spectra 3000, TeraView, U.K) was used for measuring the transmittance in the frequency range 10-1000 GHz. The setup of the transmission configuration is shown in figure (2).

Sample is placed between the THz emitter and receiver, and the THz radiation passes through it (6). The electric field vector of the received radiation is monitored as a function of time to produce a time domain spectrum (TDS). A Fourier transformation can then be used to convert this TDS to a frequency domain spectrum.

Transmittance (T) is calculated from:

$$T = \left|\frac{E_S(\omega)}{Ea\ (\omega)}\right|^2 \quad (2)$$

where Es(ω) and Ea(ω) are the complex THz electric fields passing through the sample and incident on the sample, respectively, in the frequency domain.

Total shielding effectiveness of the sample is calculated from transmittance using the relation [6]:

$$SE_{total} = -10 \log T \quad (3)$$

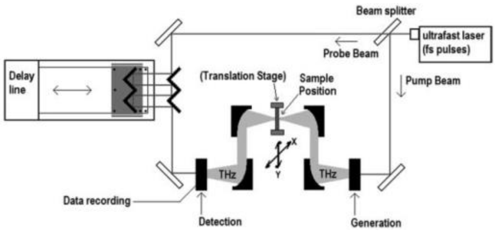

Figure (2): Configuration of a THz-TDS apparatus for transmission measurements [7].

III. Results and discussion

a) DC electric properties of CB loaded NBR composites

The effect of carbon black N220 (also known as intermediate super abrasion furnace, ISAF) on the DC electric conductivity (σ) of the filled NBR polymer is depicted in figure (3). It becomes evident that the log σ versus filler volume fraction describes S shaped relation. This behavior can be explained in light of percolation theory [8]. The percolation threshold concentration (V_{th}) could be determined graphically and was found to be 0.107 volume fraction of the CB filler. The critical volume fraction V_{cr} was determined from the plot of dlogσ/dV versus the volume fraction, which is shown in the inset of figure (3), and found to be 0.175 volume fraction of CB filler.

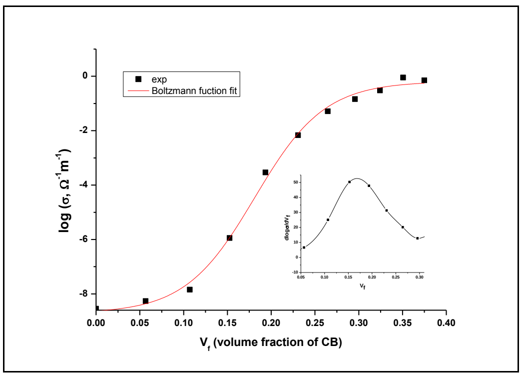

Figure (3): The variation of DC conductivity of CB loaded NBR composites (0-100 phr).

Boltzmann sigmoidal function was used for theoretical fitting of the experimental data as shown in figure (3). It has the general form:

$$\log \sigma = \log \sigma_p + \frac{\log \frac{\sigma_F}{\sigma_p}}{1+\exp -\left(\frac{V-V_{cr}}{w/2}\right)} \quad (4)$$

where σ is the conductivity of the composite, σ_F is the conductivity at the maximum packing fraction, σ_p is the conductivity of the polymer, V is the volume fraction of the filler, V_{cr} is the critical volume fraction of the filler i.e. the volume fraction in the midpoint of the percolation region, and w is the width of the percolation region i.e. $w = V_{cr} - V_{th}$.

b) I-V characteristics and DC conduction mechanism

Information about the conduction mechanism that prevails in CB loaded NBR composites can be revealed from their I-V characteristic curves. LogI - LogV plots constructed at 300K are shown in figure (4). The values of the current voltage non-linearity coefficient ($\alpha = \frac{dI}{dV}$) are enlisted in table (2). It can be easily noticed that it is mostly linear for all samples except for CB30 and CB40. These two samples were shown to follow the Mott and Gurney square law [9]:

$$J = \frac{9}{8}\varepsilon\varepsilon_o\mu\frac{V^2}{d^3} \quad (5)$$

where μ is the free carrier mobility, ε_o the permittivity of free space, ε the dielectric constant of the sample material and d is the sample thickness.

The plots of J versus V^2 for sample CB30 and CB40 give straight lines especially at high electric field as shown in the inset of figure (4).

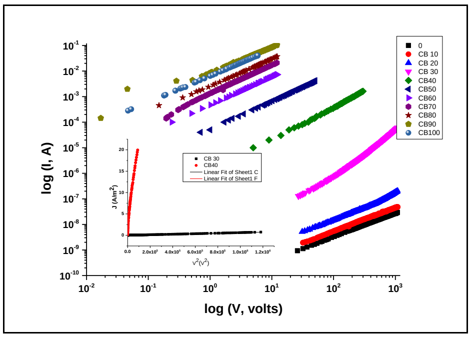

Figure (4): The I-V characteristic curves for the CB loaded NBR samples at 300K plotted on a a log- log scale. The inset shows the relation of J versus V^2 for CB30 and CB40 samples.

Figure (5) shows the variation of DC electric conductivity with electric field plotted on a log-log scale. For all samples except CB30 and CB40, DC conductivity remains nearly unchanged with increasing applied electric field. It is clear that CB30 and CB40 follow the theory of space charge limited conduction. In the case of a uniform distribution of localized states i.e. g(E)= g_o , the current I at a particular voltage V is given by the relation [10]:

$$I = \left(\frac{eA\mu n_o V}{d}\right)\exp(SV) \quad (6)$$

where d is the electrode spacing, n_o is the density of the thermally generated charge carriers, μ is the mobility, e is the electronic charge, A is the area of cross section of the sample and S is given by [11]:

$$S = \frac{2\varepsilon_r\varepsilon_o}{eg_o kTd^2} \qquad (7)$$

Where ε_r is the relative permittivity, ε_o the permittivity of free space, and T is the absolute temperature.

As evident from the above equations, a plot of log I/V vs. V for CB30 and CB40 give linear responses especially at high electric fields indicating the space charge limited conduction for these two samples. This is shown in the inset of figure (5).

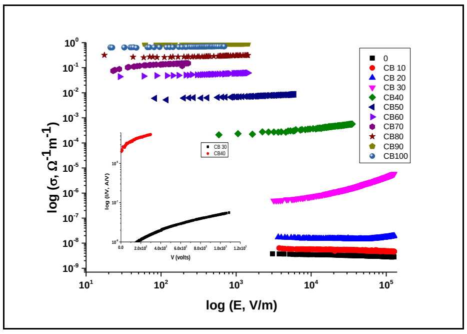

Figure (5): Variation of DC conductivity with electric field plotted on a log-log scale for CB loaded NBR samples (0-100 phr) at 300K. The inset shows the relation of log I/V versus V for CB30 and CB40 samples.

Table (2): variation of nonlinearity coefficient, and a, with CB content.

Loading level (phr)	α	a(nm)	J_o (A/ m^2)
0	0.923	14.3	0.00714
10	0.943	8.91	0.00216
20	0.951	1.71	723.4181
30	1.717	5.66	811.4811
40	1.287	1.75	85205.59
50	1.109	0.85	1.19E+06
60	1.107	0.71	198166
70	1.114	0.44	433900
80	1.076	0.24	3.84E+06
90	1.000	0.04	1.04E+09
100	1.03	0.02	1.97E+04

The current density versus electric field (J-E) behavior of the samples could also be fitted with the famous sinh equation of the form [12]:

$$J = J_o \sinh\frac{eaE}{2k_B T} \qquad (8)$$

Where J is the current density flowing through the specimen across which an electric field E is applied at a certain temperature T. J_o is the fitting parameter, e is the effective electronic charge (1.6×10^{-19}), k_B is Boltzman constant (1.38×10^{-23} Joule/K), and a is the separating distance between carbon black aggregates.

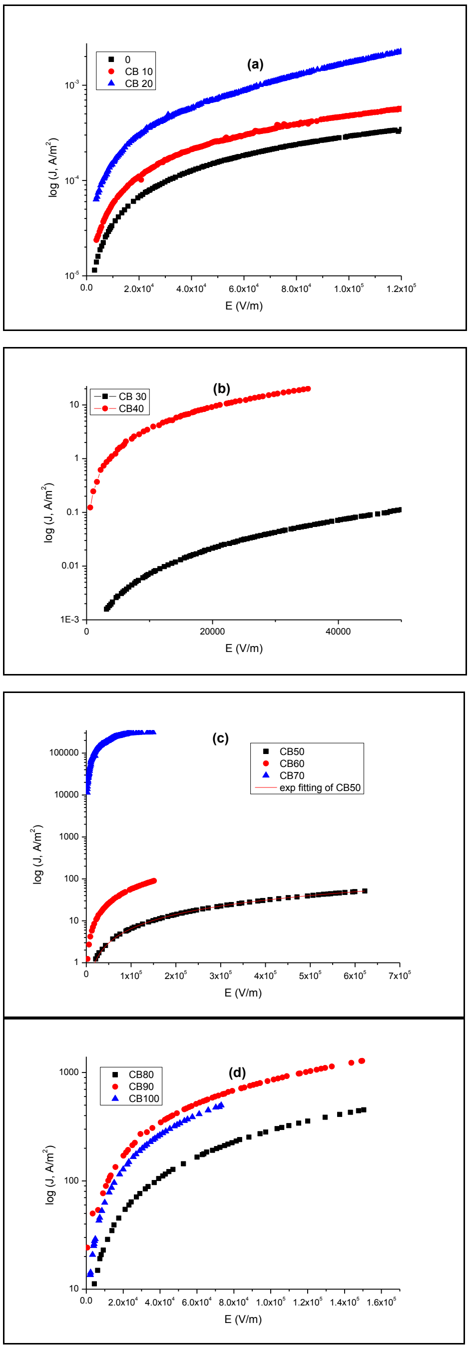

Figure (6: a,b,c,d): Variation of log J with E for CB loaded NBR composites.

Figure (6) shows the variation of log J versus E for CB loaded samples. An approximate estimate of the values of the separation distance (a) and the fitting parameter J_o were obtained numerically using an iterative method and the data are represented in table (2). One can easily notice that the interspacing separation distance (a) generally decreases appreciably with increasing CB content in CB loaded NBR composites which in turn leads to an increase in the DC electric conductivity

c) Shielding effectiveness of CB loaded NBR composites

Figure (7) shows the shielding effectiveness of CB loaded NBR composites in the frequency range 10-100 GHz. The highest possible shielding effectiveness was due to sample CB70. Recalling in mind that is the sample that was on the edge of the conducting region of the S shaped curve, figure (3), describing the evolution of DC conductivity of CB loaded NBR composites with filler concentration. Other CB loaded NBR composites show SE behavior similar to that given by the DC electric conductivity pattern.

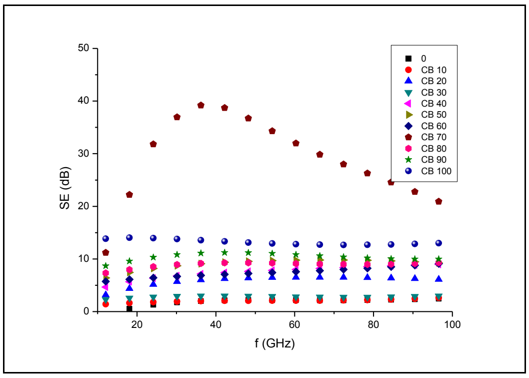

Figure (7): Shielding effectiveness for CB loaded NBR composites in the frequency range 10-100 GHz.

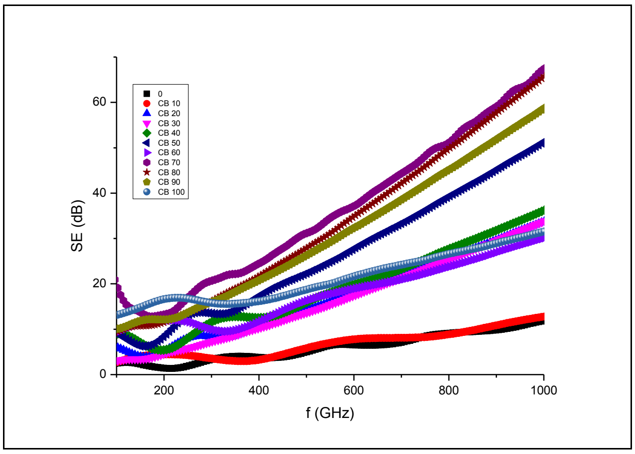

Figure (8): Shielding effectiveness for CB loaded NBR composites in the frequency range 100-1000 GHz.

Figure (8) shows the shielding effectiveness of CB loaded NBR composites in the frequency range 100-1000 GHz. CB 70 sample still leads all other CB loaded samples showing the maximum SE in this frequency range. The hierarchy of other samples might differ slightly, however they nearly preserve their ranking as in the DC electric conductivity.

One can easily notice that in the high frequency range i.e 100-1000 GHz, the shielding effectiveness increases with increasing the frequency. This can be probably ascribed to the increased shielding of microwaves by reflection due to carbon black agglomerates.

IV. Conclusion

From the forgoing results and discussion we may conclude the following:

The measurements of the electrical conductivity of CB loaded NBR composites are in compliance with the percolation theory. Percolation limit was found to be around 0.107 volume fraction of filler. Boltzmann sigmoidal model gave an excellent fit with the S-shaped conductivity versus filler content curve. All samples showed Ohmic current - voltage curves except for CB30 and CB40. The latter two samples were shown to follow the Mott and Gurney square law pointing to the prevalence of space charge limited conduction mechanism.

Microwave shielding measurements showed that CB70 sample gave the highest shielding effectiveness in both 10-100 GHz and 100-1000 GHz ranges. This was due to its high DC electric conductivity. Thus 70 phr can be considered the critical concentration in this regard and can be used in preparation of industrial microwave shielding magnetodielectric composites.

References

[1] D.D.L. Chung, JMEPEG; 9:350-354 (2000).

[2] K. Jagatheesan, A. Ramasamy, A. Das and A. Basu; Indian Journal of Fibre & Textile Research; 39 , 329-342 (2014). .

[3] R. Ou, R. A. Gerhardt, C. Marrett, A. Moulart, J. S. Colton, Composites: Part B 34, 607–614(2003).

[4] R.M. Morsy, M.N. Ismaielb and A.A. Yehia; International Journal of Materials, Methods and Technologies, 1(4) 22-35(2013).

[5] J. Arranz-Andres, N. Pulido-Gonzalez, P. Marin, A. M. Aragon, and M.L. Cerrada; Progress In Electromagnetics Research B, Vol. 48, 175-196,(2013).

[6] *Ryan M. Smith & Mark A. Arnold, Applied Spectroscopy Reviews, 46:8, 636-679, (2011)*

[7] L. REJON,A. ROSAS-ZAVALA, J. PORCAYO-CALDERON, And V. M. CASTANO, POLYMER ENGINEERING AND SCIENCE, SEPTEMBER 2000, Vol. 40, No. 9 .

[9] F. Chang, T. Li, J Matter Sci.;377:382 (2006).

[10] M. A. Lampert and M. Park, Current Injection in Solids, Acad. Press, New York, (1970).

[11] V. S. KUSHWAHA, S. KUMAR, A. KUMAR; Turk J Phys 29 (2005) , 349-354.

[12] A.R. Blythe, Electrical Properties of Polymers, Cambridge University Press, London, New York, Melbourne, (1979).